JPEDAV (2008) 29:398–404
DOI: 10.1007/s11669-008-9357-1
1547-7037 ©ASM International

Thermodynamic Optimization and Calculation of the $HoCl_3$-MCl (M = Na, K, Rb, Cs) Systems

Juan Hu, Yimin Sun, Tianyi Gao, Xiangzhen Meng, Yongxiang Yao, and Zhiyu Qiao

(Submitted June 15, 2007; in revised form July 10, 2008)

According to measured experimental phase diagram data and thermodynamic data, the $HoCl_3$-MCl (M = Na, K, Rb, Cs) phase diagrams were determined by the CALPHAD technique. The Gibbs energies of liquid phases in these systems have been optimized and calculated by the modified quasi-chemical model in the pair-approximation for short-range ordering. A series of thermodynamic functions have been optimized and calculated on the basis of an interactive computer-assisted analysis. The results show that the thermodynamic properties and phase diagrams are self-consistent. The optimized results for the systems are discussed.

Keywords modified quasi-chemical model, phase diagram, thermodynamic property

1. Introduction

Molten salts are used as fluid targets in the nuclear incineration of transuranium elements with proton accelerators. Molten salts are also used as the media in high-temperature chemical reprocessing of spent nuclear fuel from fast reactors. Molten salt electrolysis is widely used for the production of rare earth metals and their alloys.[1] Thus the phase diagrams of rare earth metal halides in combination with alkali metal halides are of prime importance for the aforementioned practical applications.

The authors used the modified quasi-chemical model in the pair-approximation for short-range ordering to optimize Gibbs energies of liquid phases and calculate thermodynamic functions. To obtain some data for thermodynamics functions without experimental data and continue our previous work,[2-9] thermodynamic optimization and calculation of the $HoCl_3$-MCl (M = Na, K, Rb, Cs) phase diagrams are reported in this paper.

2. Model

Some theoretical models of liquid solution thermodynamics such as ideal solution, regular solution, subregular solution, quasi-regular solution, and quasi-chemical theory were built to describe thermodynamic properties of liquid phases. However, it is difficult to describe the liquid phase of a binary system with strong interactions by using the above models. Pelton and Blander[10-13] modified the classical quasi-chemical theory of Fowler and Guggenheim[14,15] with short-range ordering. Instead of the real components of the system, first-nearest-neighbor pairs were used in the method. Suppose A and B are the real components in an A-B system, then three first-nearest-neighbor pairs AA, BB, and AB are considered.:

$$(A\text{-}A) + (B\text{-}B) = 2(A{-}\mathrm{B}) : \Delta g_{AB} \quad \text{(Eq 1)}$$

where (i-j) represents a first-nearest-neighbor pair. With n_A and n_B being the respective number of moles of A and B, the mole fractions, X_A and X_B, are

$$X_A = n_A/(n_A + n_B) = 1 - X_B \quad \text{(Eq 2)}$$

To transform to a system of strongly coordinated pairs, coordination-equivalent fractions Y_A and Y_B of the pairs are defined as:

$$\begin{aligned} Y_A &= Z_A n_A/(Z_A n_A + Z_B n_B) \\ &= Z_A X_A/(Z_A X_A + Z_B X_B) \\ &= 1 - Y_B \end{aligned} \quad \text{(Eq 3)}$$

Now the pair fraction X_{ij} is defined as:

$$X_{ij} = n_{ij}/(n_{AA} + n_{BB} + n_{AB}) \quad \text{(Eq 4)}$$

Here n_{ij} is the number of moles of (i-j) pairs, and Z_A and Z_B are the coordination numbers of A and B. Z_{ij} is the coordination number of i-j pairs.

$$Z_A n_A = 2n_{AA} + n_{AB} \quad \text{(Eq 5)}$$

$$Z_B n_B = 2n_{BB} + n_{AB} \quad \text{(Eq 6)}$$

$$\frac{1}{Z_A} = \frac{1}{2n_{AA} + n_{AB}}\left(\frac{2n_{AA}}{Z^A_{AA}} + \frac{n_{AB}}{Z^A_{AB}}\right) \quad \text{(Eq 7)}$$

Juan Hu, Yimin Sun, Tianyi Gao, Xiangzhen Meng, and **Yongxiang Yao**, College of Chemistry and Materials Science, Anhui Normal University, No. 1, Beijing East Road, Wuhu City, Anhui Province 241000, P.R. China; and **Zhiyu Qiao**, Department of Physical Chemistry, University of Science and Technology Beijing, Beijing 100083, P.R. China. Contact e-mail: mysun@mail.ahnu.edu.cn.

$$\frac{1}{Z_B} = \frac{1}{2n_{BB} + n_{AB}} \left(\frac{2n_{BB}}{Z^B_{BB}} + \frac{n_{AB}}{Z^B_{AB}} \right) \quad \text{(Eq 8)}$$

Substitution of Eq 5 and 6 into 3 and 4 gives

$$Y_A = X_{AA} + X_{AB}/2 \quad \text{(Eq 9)}$$

$$Y_B = X_{BB} + X_{AB}/2 \quad \text{(Eq 10)}$$

The molar pair Gibbs energies of *i-j* pairs, that is, g^0_{AA}, g^0_{BB}, and g^0_{AB} are defined according to:

$$g^0_{AA} = \frac{2g^0_A}{Z_{AA}}, \quad g^0_{BB} = \frac{2g^0_B}{Z_{BB}} \quad \text{(Eq 11)}$$

$$g^0_{AB} = \Delta g^0_{AB} + g^0_{AA}\frac{Z_{AA}}{Z_{AB}} + g^0_{BB}\frac{Z_{BB}}{Z_{BA}} = \Delta g^0_{AB} + \left(\frac{2g^0_A}{Z_{AB}} + \frac{2g^0_B}{Z_{BA}} \right) \quad \text{(Eq 12)}$$

Then the Gibbs energies of the solution is given by

$$G = n_A g^0_A + n_B g^0_B - T\Delta S^{\text{config}} + (n_{AB}/2)\Delta g_{AB} \quad \text{(Eq 13)}$$

where g^0_A and g^0_B are the molar Gibbs energies of the pure components, and ΔS^{config} is the configurational entropy of mixing given by randomly distributing the (*A-A*), (*B-B*), and (*A-B*) pairs.

$$\Delta S^{\text{config}} = -R(n_A \ln X_A + n_B \ln X_B) - R\left(n_{AA} \ln \frac{X_{AA}}{Y^2_A} + n_{BB} \ln \frac{X_{BB}}{Y^2_B} + n_{AB} \ln \frac{X_{AB}}{2Y_A Y_B} \right) \quad \text{(Eq 14)}$$

The Gibbs energies of the *A-B* system are given by:

$$G = (n_A g^0_A + n_B g^0_B) + RT(n_A \ln X_A + n_B \ln X_B) + RT\left(n_{AA} \ln \frac{X_{AA}}{Y^2_A} + n_{BB} \ln \frac{X_{BB}}{Y^2_B} + n_{AB} \ln \frac{X_{AB}}{2Y_A Y_B} \right) + \frac{n_{AB}}{2}\Delta g_{AB} \quad \text{(Eq 15)}$$

Δg_{AB} is the molar energy of *A-B* pairs, which is a function of mole fractions of the *i-j* pairs and can be expressed as:

$$\Delta g_{AB} = \Delta g^0_{AB} + \sum g^i_{AB} X^i_{AA} + \sum g^j_{AB} X^j_{BB} \quad \text{(Eq 16)}$$

or

$$\Delta g_{AB} = \Delta g^0_{AB} + \sum g^{ij}_{AB} X^i_{AA} X^j_{BB} \qquad (i + j \geq 1) \quad \text{(Eq 17)}$$

For Eq 16 and 17, $i + j \geq 1$; in practice we will always have either $i = 0$ or $j = 0$.

3. Experimental Data

Seifert and Sandrock determined the phase diagram of $HoCl_3$-NaCl system using DTA and high-temperature XRD.[16] There are three compounds Na_3HoCl_6, $NaHoCl_4$, and $NaHo_2Cl_7$. In the 1960s, Korshunov et al.[17] measured the phase diagram of $HoCl_3$-KCl system. Two congruently melting compounds K_3HoCl_6 and KHo_2Cl_7 were confirmed. The melting points (T_m) of $HoCl_3$ and KCl are 991 and 1047 K, respectively. Experimental dots and data of critical points were not shown in the phase diagram, so the authors did not choose it. Later, Roffe and Seifert investigated $HoCl_3$-MCl (M = K, Rb, Cs) systems by DTA and XRD.[18] The existence of compounds M_3HoCl_6, Cs_2HoCl_5, $Cs_3Ho_2Cl_9$, and MHo_2Cl_7 were confirmed. Additionally, the 2:1 compounds Rb_2HoCl_5 and K_2HoCl_5 were found.

The thermodynamic functions for the formation from $HoCl_3$ and MCl and for the formation from the compounds adjacent in the phase diagrams were measured by solution calorimetry and emf versus *T* measurements in galvanic chloride cells for solid electrolytes. These data are shown in later tables that compare experimental and calculated data.

4. Optimization and Calculation Results

Before calculating the phase diagrams, the coordination numbers Z_{ij} should be determined first. For the binary rare earth halide systems, Z_{AA} and Z_{BB} both equal 6 experientially.[19] In the $HoCl_3$-MCl systems, there is a tendency to form the compound $HoCl_3 \cdot 3MCl$, for example, Na_3HoCl_6, K_3HoCl_6, Rb_3HoCl_6, Cs_3HoCl_6. So in the pair *A-B*, Z_{AA}:Z_{BB} is 3:1. The ratio remains unchanged in the calculation. Therefore, the coordination numbers are accepted as $Z_{MM} = 6$, $Z_{HoHo} = 6$, $Z_{MHo} = 2$, and $Z_{HoM} = 6$.

4.1 Thermodynamic Properties of Pure Components

All thermodynamic data for the pure components at 298.15 K come from the FACTBASE[20] and USEBASE (Table 1), in which the authors stored the latest published thermodynamic data. Gibbs energy, enthalpy, entropy, and thermal capacity at some temperature are expressed using:

$$C_p(\text{J/mol} \cdot \text{K}) = a + b(10^{-3})T + c(10^5)T^{-2} \quad \text{(Eq 18)}$$

$$G\ (T) = H_0 - TS_0 + \int_{298.15}^{T} CpdT - T\int_{298.15}^{T} \frac{Cp}{T}dT \quad \text{(Eq 19)}$$

$$\Delta G^0_{\text{fus}} = G^{\text{L}}(T) - G^{\text{S}}(T) \quad \text{(Eq 20)}$$

4.2 Optimized Parameters of Liquid Phases

In the present approach, the molar energy of *A-B* pairs, Δg_{AB} is function of mole fractions of *i-j* pairs shown in Eq 16 and 17. However, it has different kinds of expressions. In order to suit the form of the FACTBASE, the Margules expression (Eq 21) is used in this work:

$$\Delta g_{AB} = \sum X_{AB} X_n^j (C_1 + C_2 T) \quad \text{(Eq 21)}$$

In Eq 21 n is AA or BB, and $C_1$and C_2 are the enthalpy of mixing and the excess entropy, respectively. In these systems $C_2 = 0$ and $j = 0,1,2,4$. All the parameters of the $HoCl_3$-MCl systems are shown in Table 2.

4.3 Enthalpies of Mixing and Interaction Parameters of Mixing Enthalpy in Liquid Phases

The calculated enthalpies of mixing (ΔH) and interaction parameters $\lambda^M = \Delta H/(X_{MCl}X_{HoCl_3})$ are shown as lines in Fig. 1 and 2, respectively. In Fig. 1, one can find that the enthalpies of mixing become more negative from $HoCl_3$-NaCl to $HoCl_3$-CsCl, and the minimum values are about $X_{HoCl_3} \approx 0.4$.

Figure 2 shows the variational trend of λ^M. It is evident that the values of interaction parameters are more negative in the alkali chloride-rich range. The broad minimum values in λ^M are found at $X_{HoCl_3} \approx 0.25$. These results are in good agreement with the modified quasi-chemical model for short-range ordering.

4.4 Gibbs Energies of Mixing

Figure 3 shows the Gibbs energies of mixing at different temperature. From calculated values, we found that the

Table 1 Thermodynamic properties of pure compounds for solid and liquid state at 298.15 K

Compound	T range, K	H^0	S^0	a	b	c
NaCl (solid)	298-2,000	−411,119.8	72.132	45.940	16.318	...
NaCl (liquid)	298-1,500	−394,956.0	76.076	77.764	−7.531	...
	1,500-2,000	−390,090.1	84.505	66.944	...	...
KCl (solid)	298-2,500	−436,684.1	82.550	40.016	25.468	3.648
KCl (liquid)	298-2,500	−42,182.5	86.523	73.596	...	...
RbCl (solid)	298-2,000	−430,533.6	91.630	48.116	10.418	...
RbCl (liquid)	298-1,625	−418,498.8	98.279	64.015	...	...
CsCl (solid)	298-2,000	−441,267.3	101.214	59.731	4.937	...
CsCl (liquid)	298-2,000	−434,461.9	101.719	77.404	...	...
HoCl3 (solid)	298-993	−1,005,415.2	146.86	95.562	12.970	−0.962
HoCl3 (liquid)	298-1,100	−1,002,742.1	128.19	143.720	...	...

Table 2 Calculated coefficients of the $HoCl_3$-MCl systems

		C_1 (j = 1)		C_1 (j = 2)		C_1 (j = 4)	
System	C_1 (j = 0)	X_{AA}	X_{BB}	X_{AA}	X_{BB}	X_{AA}	X_{BB}
NaCl	−6,779.99	234.34	−3,888.87	0.0000	594.23	0.0000	0.0000
KCl	−13,991.36	444.36	−9,189.52	0.0000	−4,663.10	0.0000	0.0000
RbCl	−13,077.96	−210.07	3,014.58	−7,327.22	−5,584.27	0.0000	0.0000
CsCl	−15,194.88	−1,235.52	−1,982.63	11,597.95	−3,050.86	0.0000	0.0000

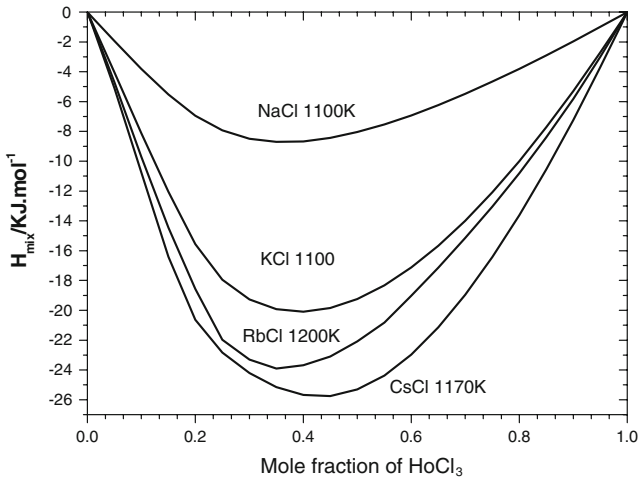

Fig. 1 Enthalpies of mixing in the $HoCl_3$-MCl systems

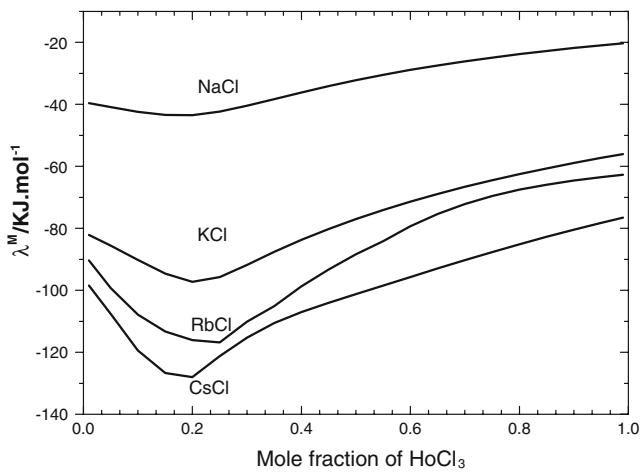

Fig. 2 Interaction parameters in the $HoCl_3$-MCl systems

variational trend of Gibbs energies of mixing is similar to of enthalpies of mixing. The minimum values are also at $X_{HoCl_3} \approx 0.4$. At the same component and temperature, the values of Gibbs energies of mixing are smaller than those of enthalpies of mixing.

4.5 Intermediate Compounds

The thermodynamic functions for the formation of intermediate compounds can be expressed by:

$$\Delta G^0_{f(A_mB_n)} = a - bT, \text{ J/ mole} \quad \text{(Eq 22)}$$

The term $\Delta G^0_{f(A_mB_n)}$ is the Gibbs energy of the formation per mol of atoms of the compounds, and where a and b are the enthalpies and entropies for the formation of all the intermediate compounds, respectively, also listed in Table 3.

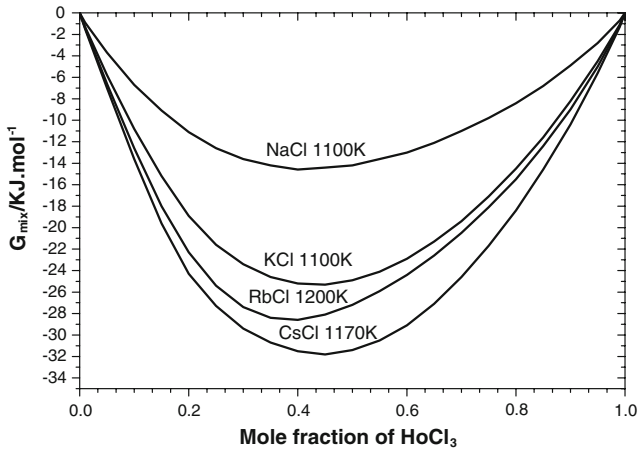

Fig. 3 Gibbs energies of mixing in the $HoCl_3$-MCl systems

Moreover, the experimental values of a are listed in Table 3 and in agreement with calculated values. The measured melting points or peritectic temperatures with (a) are also shown in Table 3. All temperatures and experimental values come from Ref 16 and 18.

4.6 Phase Diagram

All collected data were used to optimize the thermodynamic properties and phase diagrams by a simple computer program. The phase diagrams of the $HoCl_3$-MCl systems are shown in Fig. 4, 5, 6, 7; the solid lines in the figures represent the calculated data, and the dots show the experimental data. The experimental invariant points and the calculated values

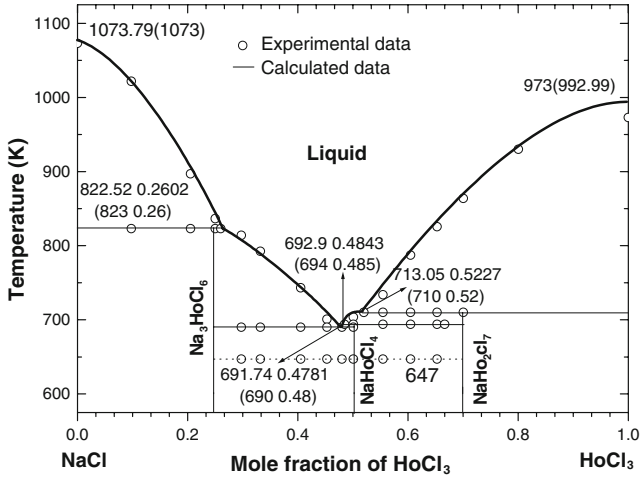

Fig. 4 The measured (○) and calculated (—) phase diagram of the $HoCl_3$-NaCl system

Table 3 Thermodynamic properties of intermediate compounds

		$\Delta G^0_{f(A_mB_n)} = a - bT$ (J/mol)			
		$a \times 10^{-3}$		$a \times 10^{-3}$	
Intermediate compound	T^0_{fus}, K	Calculated	Experimental	Calculated	Experimental
Na_3HoCl_6	823(a)	−5.22	−5.00	20.83	...
$NaHoCl_4$	694(a)	−8.86	−8.80	−2.28	...
$NaHo_2Cl_7$	710(a)	−7.00	−7.00	1.81	...
K_3HoCl_6	1077	−59.29	−53.50	66.89	...
KHo_2Cl_7	841	−54.46	−54.60	−11.69	...
Rb_3HoCl_6	1147	−76.58	−76.80	33.03	...
Rb_2HoCl_5	785(a)	−91.87	...	−23.82	...
$RbHo_2Cl_7$	886	−59.01	−65.00	27.71	...
Cs_3HoCl_6	1150	−95.00	−95.00	28.21	...
Cs_2HoCl_5	915(a)	−81.75	...	8.55	...
$Cs_3Ho_2Cl_9$	842(a)	−128.85	−128.00	17.56	...
$CsHo_2Cl_7$	913	−65.77	−65.60	5.68	...

(a) Peritectic temperature

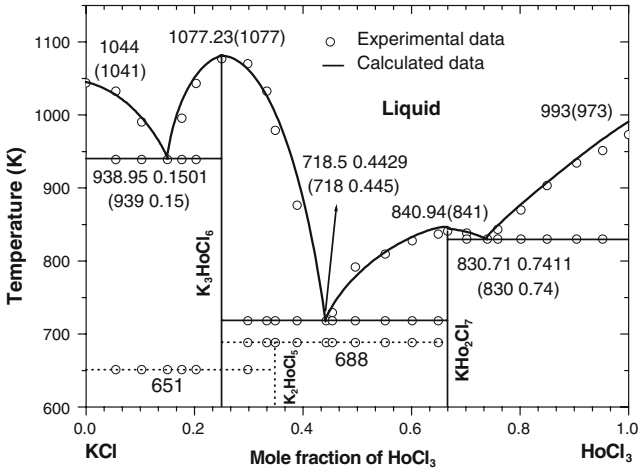

Fig. 5 The measured (○) and calculated (—) phase diagram of the $HoCl_3$-KCl system

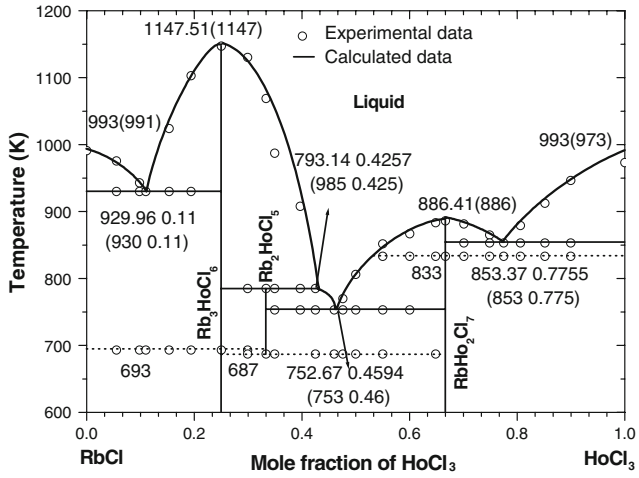

Fig. 6 The measured (○) and calculated (—) phase diagram of the $HoCl_3$-RbCl system

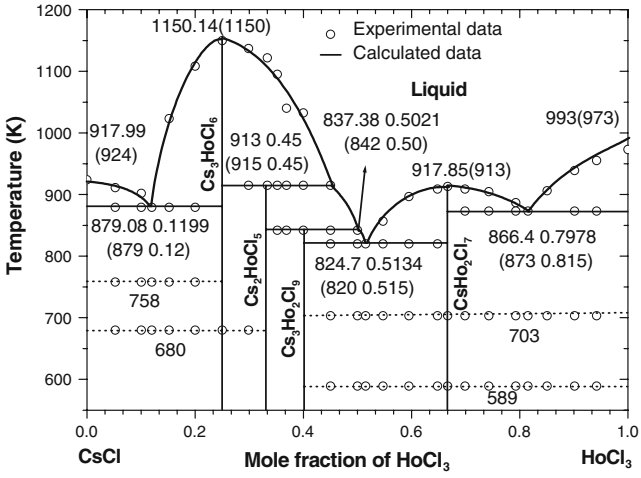

Fig. 7 The measured (○) and calculated (—) phase diagram of the $HoCl_3$-CsCl system

for the $HoCl_3$-MCl (M = Na, K, Rb, Cs) systems are shown in Table 4. Generally, the optimized data agree with experimental data. However, the melting of pure component is fixed by computer program. The calculated data of critical points are shown in figures. Dotted lines show solid-solid phase transformations.

5. Discussion

Thermodynamic properties of mixing in the liquid phase were obtained by optimization and calculation. Figures 1 and 3 show enthalpies and Gibbs energies of mixing in liquid phases. The enthalpies and Gibbs energies of mixing become more negative in the sequence from $HoCl_3$-NaCl to $HoCl_3$-CsCl with the increasing of the radius of alkali metal ion from Na^+ to Cs^+, and the $HoCl_3$-CsCl system has the largest negative value. The minimum of the enthalpies and Gibbs energies of mixing are shifted toward the alkali chloride-rich compositions and located in $X_{HoCl_3} \approx 0.4$. It is evident that the ionic radius of the alkali metal influences the magnitude of enthalpies and Gibbs energies of mixing as well as the location of minimum. The bigger the ionic radius, the smaller the mixing enthalpies and Gibbs energies, and the minimum shifted more toward the alkali chloride rich composition.

Rare earth ionic charges are higher and radii are bigger, Cl electronegativity is higher and Cl flexibility is bigger. Coulomb force, van der Waals force, and polarization exist in the molten systems simultaneously. So asymmetric interactions are reflected in the parameter, λ^M, (see Fig. 2). All the systems have negative λ^M with the degree of negativity increasing sharply with the increasing radius of the alkali metal ion and show more negative values of the interaction parameter in the alkali chloride-rich region than in the holmium chloride-rich range. Furthermore, broad minima in the composition dependence of the interaction parameters were found near $X_{HoCl_3} \approx 0.25$. Liquid phase short-range ordering sharply increase in the regions of these minima. Moreover, the interaction between the rare earth halides and alkali metal halides is stronger. This favors easier formation of compound and associated ions, for example, compounds M_3HoCl_6 (M = Na, K, Rb, Cs) and the ion $[HoCl_6^{3-}]$.

From Fig. 4 to 7 and Table 4, it can be noted that the optimized phase diagrams and the critical points are in agreement with experimental data. Especially, the differences between critical points are small, the biggest temperature difference is no more than 8 K, and mole fractions are no more than 1%. Comparing the four phase diagrams, we found the number and stability of the compounds to increase with increasing ionic radius of the alkali metal. Because the radius of Ho^{3+} (89.4 pm) is smaller than the radii of alkali ions (102, 138, 152, and 167 for Na^+, K^+, Rb^+, and Cs^+, respectively) and its charge is three times greater than that of alkali ions, the polarization of Ho^{3+} versus Cl^- is stronger and the antipolarization of M^+ trends weaker from Na^+ to Cs^+. Consequently in the systems, negative deviations from ideal solutions become bigger and bigger from Na^+ to Cs^+.

Table 4 Invariant temperatures and compositions for the $HoCl_3$-MCl binary systems

System	Reaction	Calculated values		Experimental values		Type
		T, K	Composition, mol% $HoCl_3$	*T*, (K)	Composition, mol% $HoCl_3$	
$HoCl_3$-NaCl	$L + NaCl \leftrightarrow Na_3HoCl_6$	822.52	26.02	823	26.00	Peritectic
	$L \leftrightarrow Na_3HoCl_6 + NaHoCl$	691.74	47.81	690	48.00	Eutectic
	$L + NaHo_2Cl_7 \leftrightarrow NaHoCl_4$	692.90	48.43	694	48.50	Peritectic
	$L + ErCl_3 \leftrightarrow NaHo_2Cl_7$	713.05	52.27	710	52.00	Peritectic
$HoCl_3$-KCl	$L \leftrightarrow KCl + K_3HoCl_6$	938.95	15.01	939	15.00	Eutectic
	$L \leftrightarrow K_3HoCl_6$	1077.23	(25.00)	1077	(25.00)	Congruent point
	$L \leftrightarrow K_3HoCl_6 + KHo_2Cl_7$	718.50	44.29	718	44.30	Eutectic
	$L \leftrightarrow KHo_2Cl_7$	840.95	(66.7)	841	(66.7)	Congruent point
	$L \leftrightarrow HoCl_3 + KHo_2Cl_7$	830.71	74.11	830	74.00	Eutectic
$HoCl_3$-RbCl	$L \leftrightarrow RbCl + Rb_3HoCl_6$	929.96	11.00	930	11.00	Eutectic
	$L \leftrightarrow Rb_3HoCl_6$	1147.51	(25.00)	1147	(25.00)	Congruent point
	$L + Rb_3HoCl_6 \leftrightarrow Rb_2HoCl_5$	793.14	42.57	785	42.50	Peritectic
	$L \leftrightarrow Rb_2HoCl_6 + RbHo_2Cl_7$	752.67	45.94	753	46.00	Eutectic
	$L \leftrightarrow RbHo_2Cl_7$	886.41	(66.67)	861	(66.67)	Congruent point
	$L \leftrightarrow HoCl_3 + RbHo_2Cl_7$	853.37	77.55	853	77.50	Eutectic
$HoCl_3$-CsCl	$L \leftrightarrow CsCl + Cs_3HoCl_6$	879.08	11.99	879	12.00	Eutectic
	$L \leftrightarrow Cs_3HoCl_6$	1150.14	(25.00)	1150	(25.00)	Congruent point
	$L + Cs_3HoCl_6 \leftrightarrow Cs_2HoCl_5$	913.33	45.07	915	45.00	Peritectic
	$L + Cs_2HoCl_5 \leftrightarrow Cs_3Ho_2Cl_9$	837.38	50.21	842	50.00	Peritectic
	$L \leftrightarrow Cs_3Ho_2Cl_9 + CsHo_2Cl_7$	824.70	51.31	820	51.50	Eutectic
	$L \leftrightarrow CsHo_2Cl_7$	917.85	(66.67)	913	(66.67)	Congruent point
	$L + HoCl_3 \leftrightarrow CsHo_2Cl_7$	866.40	79.78	873	81.50	Eutectic

So it is beneficial to form intermediate compounds. For example, compound M_3HoCl_6 gradually becomes more stable and T_m increases step by step. For Rb_3HoCl_6 and Cs_3HoCl_6, T_m is far higher than the T_m of the pure components (RbCl, CsCl, and $HoCl_3$).

6. Summary

Using CALPHAD technique, the phase diagrams and thermodynamic data in the systems were critically estimated. Generally, the optimized phase boundaries agree with experimental data. The calculated enthalpy and interaction parameter are reasonable. All show that the optimized phase diagrams and calculated thermodynamic parameters are thermodynamically self-consistent.

Acknowledgments

The project is supported now by Key Project Foundation of Natural Science of Anhui Education Committee numbered as 2005KJ016ZD and the new project program not numbered yet also by Key Project Foundation of Natural Science of Anhui Education Committee and the new project program not numbered yet by Anhui Provincial Foundation of Natural Science. The authors are grateful to Canadian Science Foundation and Professor A.D. Pelton's research group in Montreal University, Canada for their helpful suggestion. The authors are also grateful to Professor H.J. Seifert from whom we get the experimental data of phase diagram.

References

1. Z. Qiao, W. Zhuang, and M. Sun, Thermodynamic Analysis of the Binary ACl-YCl_3 (A: Li, Na, K, Rb, Cs) Phase Diagrams, *Sci. China*, 1992, **2**, p 171-177, in Chinese
2. Z. Ma, Y. Sun, Y. Ding, Y. Wang, and Z. Qiao, Thermodynamic Calculation of $GdCl_3$-MCl (M = Na, K, Rb, Cs) Phase Diagrams Based on Experimental Data, *Calphad*, 2006, **30**, p 88-94
3. Y. Wang, Y. Sun, Z. Qiao, X. Ye, Z. Ma, and X. Meng, Thermodynamic Optimization and Calculation of the $SmCl_3$-MCl (M = Na, K, Rb, Cs) Phase Diagrams, *Calphad*, 2005, **29**, p 317-322
4. Y. Sun, Z. Ma, Y. Ding, Y. Wang, and Z. Qiao, Optimization and Calculation of the $EuCl_3$-MCl (M = Na, K, Rb, Cs) Phase Diagrams, *J. Solution Chem.*, 2005, **34**(10), p 1197-1209
5. Y. Sun, Y. Wang, Z. Ma, X. Meng, X. Ye, and Z. Qiao, Thermodynamic Optimization of the Binary $YbCl_3$-$AECl_2$ (AE = Mg, Ca, Sr, Ba) Systems, *J. Phase Equilib. Diff.*, 2005, **26**(6), p 616-621
6. Y. Sun, X. Ye, Y. Wang, and J. Tan, Optimization and Calculation of the $NdCl_3$-MCl (M = Li, Na, K, Rb, Cs) Phase Diagrams, *Calphad*, 2004, **28**, p 109-114
7. X. Ye, J. Zhang, Y. Wang, and Y. Sun, Optimization and Calculation of the $LaBr_3$-MBr (M = Na, K, Rb, Cs) Phase Diagrams, *Calphad*, 2004, **28**, p 147-151

8. J. Zhang, Y. Sun, M. Guan, and Z. Qiao, Thermodynamic Optimization of the $CeCl_3$-$AECl_2$ (AE = Mg, Ca, Sr, Ba) Phase Diagrams, *Calphad*, 2003, **27**, p 305-308
9. Y. Sun, J. Zhang, M. Guan, and Z. Qiao, Optimization and Calculation of $TbCl_3$-ACl (A = Li, Na, K, Rb, Cs) Phase Diagrams, *J. Rare Earths*, 2005, **1**, p 27-31
10. M. Blander and A.D. Pelton, Thermodynamic Analysis of Binary Liquid Silicates and Prediction of Ternary Solution Properties by Modified Quasichemical Equations, *Geochim. Cosmochim. Acta*, 1987, **51**(1), p 85-95
11. A.D. Pelton, S.A. Degterov, G. Eriksson, C. Robelin, and Y. Dessureault, The Modified Quasichemical Model I-Binary Solutions, *Metall. Mater. Trans.*, 2000, **31B**, p 651-659
12. A.D. Pelton and M. Blander, Analysis and Prediction of the Thermodynamic Properties of Multicomponent Silicates, *Proc. AIME Symposium on Molten Salts and Slags* (Lake Tahoe, NV), TMS-AIME, Warrendale, PA, 1984, p 281-294
13. A.D. Pelton and M. Blander, Thermodynamic Analysis of Ordered Liquid Solutions by a Modified Quasichemical Approach Application to Silicates Slags, *Metall. Trans.*, 1986, **17B**(4), p 805-815
14. R.H. Fowler and E.A. Guggenheim, *Statistical Thermodynamics*, Cambridge University Press, Cambridge, UK, 1939, p 350-366
15. E.A. Guggenheim, The Statistical Mechanics of Regular Solutions, *Proc. R. Soc.*, 1935, **A148**, p 304-312
16. H.J. Seifert and J. Sandrock, Ternary Chlorides in the Systems NaCl/$HoCl_3$ and NaCl/$ErCl_3$, *Z. Anorg. Allg. Chem.*, 1997, **623**, p 1525-1528
17. B.G. Korshunov, D.V. Drobot, I.E. Gachenko, and Z.X. Shevtsova, *Zh. Neorg. Khim.*, **11**(2), 1966, p 411, in Russian; *J. Inorg. Chem.* (English transl), 1966, **224**
18. M. Roffe and H.J. Seifert, Ternary Chlorides in the Systems ACl/$HoCl_3$ (A = Cs, Rb, K), *J. Alloys Compd.*, 1997, **257**, p 128-133
19. Y.M. Sun, "Measurement, Calculation and Evaluation by Pattern Recognition of the Rare Earth Halide Phase Diagrams," Dissertation of Doctor's Degree, Department of Physical Chemistry, University of Science & Technology Beijing, People's Republic of China, 1999, in Chinese
20. C.W. Bale, A.D. Pelton, and W.T. Thompson, *F*A*C*T*-Facility for the Analysis of Chemical Thermodynamic*, User's Guide and Supplement, McGill University and Ecole Polytechnique, Montreal, 1999